Rotational dynamics of proteins from spin relaxation rates and molecular dynamics simulations

O. H. Samuli Ollila*
Insititute of Biotechnology, University of Helsinki
(Dated: May 2, 2017)

I. INTRODUCTION

II. METHODS

A. Spin relaxation analysis from MD simulations

Experimentally measurable spin relaxation rates R_1, R_2 and R_{NOE} for N-H bonds are related to the molecular dynamics through equations [**?** **?**]

$$R_1 = \frac{d_{\mathrm{NH}}^2 N_{\mathrm{H}}}{20}\Big[J(\omega_{\mathrm{H}}-\omega_{\mathrm{N}}) + 3J(\omega_{\mathrm{N}}) + 6J(\omega_{\mathrm{N}}+\omega_{\mathrm{H}})\Big] + \frac{(\sigma\omega_{\mathrm{N}})^2}{15} j(\omega_{\mathrm{N}}), \tag{1}$$

$$R_2 = \frac{1}{2}\frac{d_{\mathrm{NH}}^2 N_{\mathrm{H}}}{20}\Big[4J(0) + 3j(\omega_{\mathrm{N}}) + J(\omega_{\mathrm{H}}-\omega_{\mathrm{N}}) + 6J(\omega_{\mathrm{H}}) + 6J(\omega_{\mathrm{N}}+\omega_{\mathrm{H}})\Big] + \frac{(\sigma\omega_{\mathrm{N}})^2}{15*6}[4J(0)+3J(\omega_{\mathrm{N}})], \tag{2}$$

$$R_{\mathrm{NOE}} = 1 + \frac{d_{\mathrm{NH}}^2 N_{\mathrm{H}}}{20}\Big[6J(\omega_{\mathrm{N}}+\omega_{\mathrm{H}}) + J(\omega_{\mathrm{H}}-\omega_{\mathrm{N}}))\Big]\frac{\gamma_{\mathrm{H}}}{\gamma_{\mathrm{N}} R_1}, \tag{3}$$

where ω_{N} and ω_{H} are the Larmor angular frequencies of ^{15}N and ^{1}H respectively, N_{H} is the number of bound protons. The dipolar coupling constant is given by

$$d_{\mathrm{NH}} = -\frac{\mu_0 \hbar \gamma_{\mathrm{H}} \gamma_{\mathrm{N}}}{4\pi \langle r_{\mathrm{CN}}^3 \rangle},$$

where μ_0 is the magnetic constant or vacuum permeability, $\hbar$ is the reduced Planck constant, γ_{N} and γ_{H} are the gyromagnetic constants of ^{13}C and ^{1}H, respectively, and $\langle r_{\mathrm{CN}}^3 \rangle$ is the average cubic length of the C–H chemical bond. Chemical shift anisotropy is approximately $\Delta\sigma = 160 * 10^{-6}$ for N-H bonds in proteins [**?**]. Spectral density $J(\omega)$ is defined as the Fourier transformation of the second order rotational correlation function for N-H bond

$$C(t) = \langle P_2(\theta) \rangle, \tag{4}$$

where $P_2(\theta) = (3 * \cos^2\theta - 1)/2$ is the second order Legendre polynomial. The rotational correlation function is often separated to overall and internal motions of the molecule. Assuming that these are independent one can write

$$C(t) = C_I(t) C_O(t), \tag{5}$$

where $C_i(t)$ and $C_o(t)$ are correlation functions for internal and overall rotiations, respectively. The internal correlation function decays to a plateau, which is used to defined a order parameter respect to molecular axes S^2. The internal correlation function can be then written by using reduced correlation function $C'(t)$

$$C(t) = [C_I'(t)(1-S^2) + S^2] C_O(t). \tag{6}$$

The effective correlation time describing relaxation of internal processes is then defined as

$$\tau = \int_0^\infty g'(\tau) \mathrm{d}t. \tag{7}$$

Fully anisotropic overall rotation can be described as a sum of five exponentials

$$C_O(t) = \sum_{j=1}^{5} A_j e^{-t/\tau_j}, \tag{8}$$

where $\tau_1 = (4D_{xx} + D_{yy} + D_{zz})^{-1}$, $\tau_2 = (D_{xx} + 4D_{yy} + D_{zz})^{-1}$, $\tau_3 = (D_{xx} + D_{yy} + 4D_{zz})^{-1}$, $\tau_4 = [6(D + (D^2 - L^2)^{-1/2}]^{-1}$, $\tau_5 = [6(D - (D^2 - L^2)^{-1/2}]^{-1}$, $D = \frac{1}{3}(D_{xx} + D_{yy} + D_{zz})$ and $L^2 = \frac{1}{3}(D_{xx}D_{yy} + D_{xx}D_{zz} + D_{yy}D_{zz})$. The diffusion constants around three principal axes of a molecule D_{xx}, D_{yy} and D_{zz} are are defined as

$$\begin{aligned} \langle(\Delta\alpha)^2\rangle &= 2D_{xx}t \\ \langle(\Delta\beta)^2\rangle &= 2D_{yy}t \\ \langle(\Delta\gamma)^2\rangle &= 2D_{zz}t. \end{aligned} \tag{9}$$

Standard analyses of experimental relaxation data usually assume fully or axially isotropic overall rotational motion and single decay constant for interal motion. Then the free parameters (S^2, τ_j, A_j) are fit against spin relaxation data from experiments. This gives most likely very good results for isotropic molecules for which the assumption of single internal motional timescale is reasonable. However, for molecules with significant shape anisotropy or several timescales in internal motions the amoount parameters to be fitted becomes large compared with the typical amount of experimental points.

On the other hand, trajectories of individual atoms can be calculated from classical molecular dynamics simulations. The rotational correlation functions can be calculated from

* samuli.ollila@helsinki.fi; Department of Neuroscience and Biomedical Engineering, Aalto University

such trajectories and the internal and overall rotational motions can be explicitly separated. If molecular dynamics simulation model reproduces experimental spin relaxation rates, it can be used to interpret the different dynamical processes present in the system.

The following steps are performed in practise.
1) Total rotational correlation functions $C(t)$ for protein N-H bonds are calculated from MD simulation trajectory. The rotational correlation functions for internal dynamics $C_I(t)$ are calculated from a trajectory from where the overall rotation of protein is removed. The rotation is removed by using fit option in gmx trjconv and rotational correlation functions are calculated with gmx rotacf.
2) The overall and internal motions are assumed independent. Overall rotational correlation function can be then calculated from Eq. ref?? $C_O(t) = C(t)/C_I(t)$.
3) The protein axes of intertia and their root mean square deviations as function of time are calculated from MD simulation trajectory.
4) Rotational diffusion constants D_x, D_y and D_z are calculated by fitting a straight line to root mean square angle deviations of intertia axes.
5) The weighting factors A_j are calculated by fitting Eqs. ref?? in rotational correlation functions of overall rotational motion $C_0(t)$.
6) The rotational diffusion constants are divided by the scaling factor and new overall rotational correlation functions are calculated from Eq. ref by using weights from previous step. New total correlation functions are calculated by multiplying $C_I(t)$ from simulations with new overall correlation functions.

B. Molecular dynamics simulations

Simulations were ran using Gromacs 5 [**?**] and Amber ?? force field for proteins [**?**]. The proteins were solvated to tip3p[**?**], tip4p [**?**] or OPC4 [**?**] water models. Temperature was coupled to desired value with ?? and pressure was isotropically set to 1 bar using ??. The simulated systems are listed in Table **??**

NMR structures from [**?**] and [**?**] are used as initial structure for PaTonB and HpTonB-92, respectively.

TABLE I. Systems simulated in this work.

Protein	Water model	T (K)	t_{sim} (ns)	t_{anal} (ns)	files
PaTonB	tip4p	298	?	?	[**?**]
PaTonB	tip4p	?	400	390	[**?**]
PaTonB	OPC4	?	1200		[**?**]
HpTonB-92	tip3p				[**?**]
HpTonB-92	tip4p				[**?**]
HpTonB-92	OPC4				[**?**]

III. RESULTS AND DISCUSSION

A. Protein overall rotational diffusion constants and relaxation times

Rotational correlation functions calculated from molecular dynamics simulation are shown in Fig. 1.

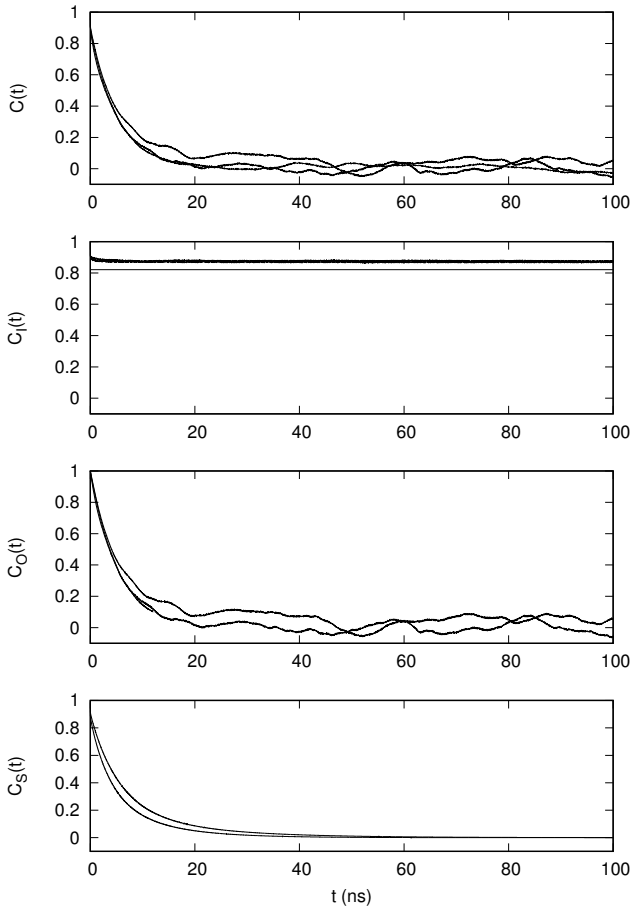

FIG. 1. Example correlation functions from residue 269 of PsTonB simulated with OPC water model. Total correlation function $g(t)$ on (top). Correlation function for internal motions calculated from trajectory from which overall rotation of protein is removed. The plateau of this gives the order paramater square S^2.

The intertia tensor angles as a function of time and mean square angular deviations are shown in Fig. 2

B. Protein internal relaxation

Fourier transform of the total correlation function $g(t)$ gives spectral density $J(\omega)$, which can be then embedded in Eqs. ?? to calculate the experimentally measurable spin relaxation rates. If MD results agree with experiments, the simulation can be used intepret the experimental data.

The analysis method is demonstrated here for HpTonB short construct. The calculated spin lattice relaxation times

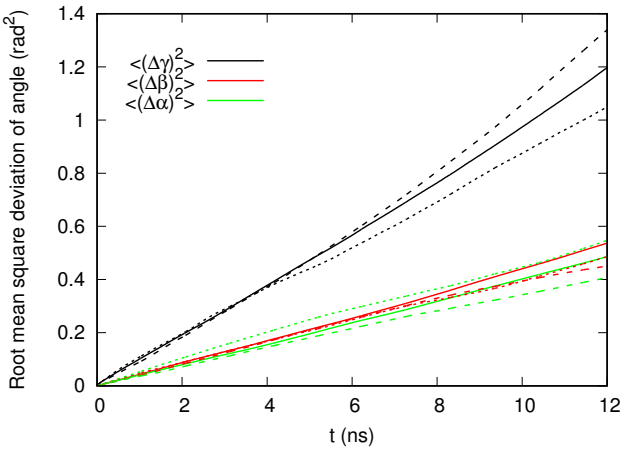

FIG. 2. The intertia tensor angles as a function of time and mean square angular deviations for PsTonB simulation with OPC water model.

TABLE II. Rotational diffusion coefficients calculated for PsTonB.

rad^2/ns	TIP4P	OPC
D_{xx}	0.026	0.020
D_{yy}	0.022	0.022
D_{zz}	0.049	0.048
$D_{\|}/D_{+}$	2.04	2.31
D_{av}	0.03	0.030
tau1	5.67	6.70
tau2	6.05	6.47
tau3	4.06	4.29
tau4	3.45	3.57
tau5	9.83	12.87

from simulations with different water models together with experimental data [**?**] are shown in Fig. 6. The rotational diffusion constants for overall

TABLE III. Rotational diffusion coefficients calculated directly from simulations in 303K. OPC RESULTS TO BE CHECKED.

rad^2/ns	TIP3P	TIP4P	OPC
D_{xx}	0.083	0.038	0.030
D_{yy}	0.077	0.033	0.027
D_{zz}	0.16	0.059	0.058
$2D_{zz}/(D_{xx}+D_{yy})$	1.99	1.7	2.03
D_{av}	0.11	0.043	0.038
tau1	1.76	4.13	4.87
tau2	1.82	4.40	5.14
tau3	1.26	3.25	3.47
tau4	1.05	2.75	2.94
tau5	3.05	6.48	8.43

Results with rotational diffusion coefficient corrected with constant factor are shown in Fig. 7.

TABLE IV. Rotational diffusion coefficients scaled with constant factor which gives a good agreement for spin relaxation data, 3.0 for tip3p simulation and by 1.3 for tip4p simulation. OPC RESULTS TO BE CHECKED.

rad^2/ns	TIP3P	TIP4P
D_{xx}	0.028	0.029
D_{yy}	0.026	0.025
D_{zz}	0.053	0.045
$2D_{zz}/(D_{xx}+D_{yy})$	1.99	1.7
D_{av}	0.034	0.033

IV. RESULTS FOR PSTONB

ACKNOWLEDGMENTS

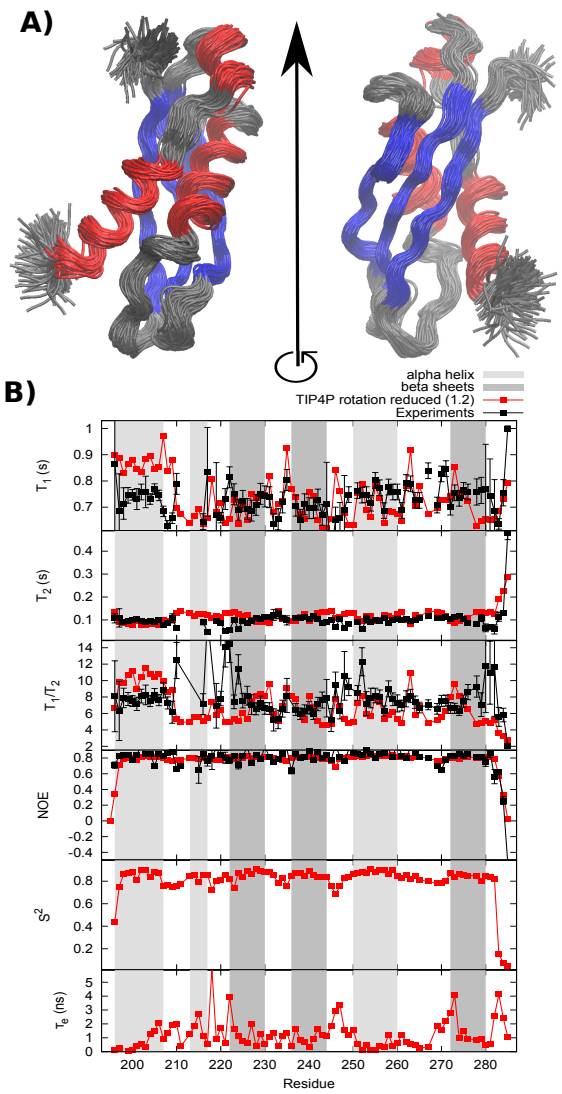

FIG. 3. A) Structures sampled by HpTonB-92 from MD simulations (100 structures from 300ns long trajectory). B) Spin relaxation rates, order parameters and effective correlation times for internal protein dynamics from experiments and simulations.

TABLE V. Rotational diffusion coefficients of inertia axes for different proteins based on MD analysis of NMR relaxation data. HpTonB-107 has slighlty slower rotational diffusion and larger anisotropy than HpTonB-92, but difference is not very large. PsTonB has slower rotational diffusion and larger anisotropy than HpTonB constructs.

rad^2/ns	HpTonB-92	HpTonB-107	PsTonB
D_{xx}	0.027 ± 0.001	0.020 ± 0.001	0.015 ± 0.001
D_{yy}	0.027 ± 0.001	0.027 ± 0.001	0.017 ± 0.001
D_{zz}	0.055 ± 0.005	0.050 ± 0.004	0.039 ± 0.001
$2D_{zz}/(D_{xx}+D_{yy})$	2.0 ± 0.2	2.2 ± 0.1	2.40 ± 0.01
D_{av}	0.036 ± 0.003	0.033 ± 0.002	0.024 ± 0.001
τ_c(ns)	4.6 ± 0.4	5.1 ± 0.3	7.1

SUPPLEMENTARY INFORMATION

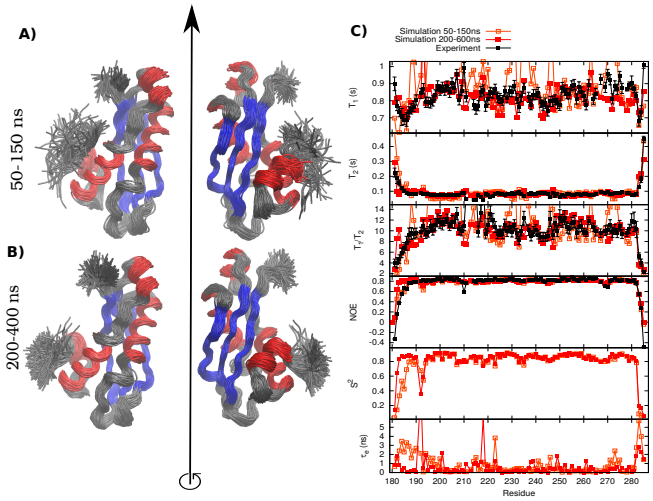

FIG. 4. A) Structures sampled by HpTonB-107 from MD simulations (100 structures from 100ns long trajectory between 50ns-150ns). B) Structures sampled for HpTonB-107 from MD simulations (100 structures from 200ns long trajectory between 200ns-400ns). C) Spin relaxation rates, order parameters and effective internal correlation times from experiments and simulations. Flexibilty observed in N terminus between residues 181-186 is better described by the dynamical model given by MD simulation between 50ns-150ns. In this model the flexible region (residues 181-186) is characterized by longer τ_e and smaller order parmameter. This means larger conformational space sampled and larger entropy. In addition, the N-terminus part missing from short construct (92-107) interacts with residues where chemical shift differences between short and longer construct were observed.

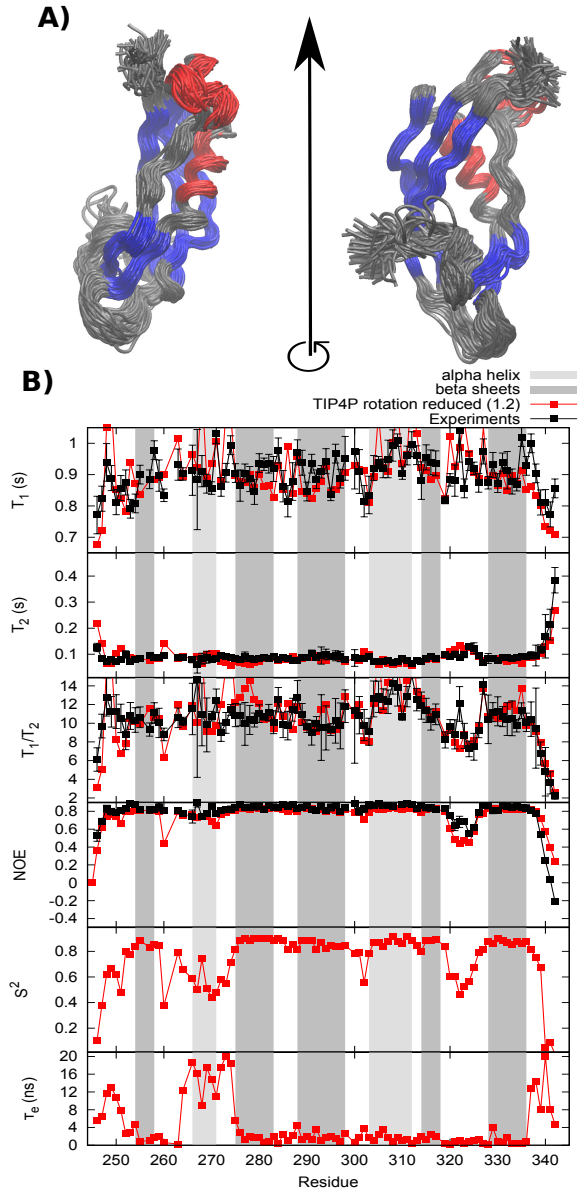

FIG. 5. A) Structures sampled by PsTonB from MD simulations (100 structures from 400ns long trajectory). B) Spin relaxation rates, order parameters and effective internal correlation times from experiments and simulations. Spin relaxation rates indicate increased flexibility only for the last two residues in N terminus. However, MD simulations suggest somewhat smaller order parameters and longer τ_e for residues 246-253. By looking at the sampled structures, it seems that lower order parameters and longer correlation times arise from slower and less extensive conformational sampling than in HpTonB-107. Lower order parameters and larger correlation times are also observed in PsTonB simulations between residues 265-275. This can be explained by the changes in orientation of alpha helix close to this region, as seen in the sampled conformations. Such effect was not seen in the HpTonB simulations, however, NMR data for this region showed some unclarities which may arise from such conformational exchange. Enhanced sampling is also observed between residues 320-326. This was not observed in HpTonB samples, which may be related to the formation of beta sheet between residues 315-318 in PsTonB.

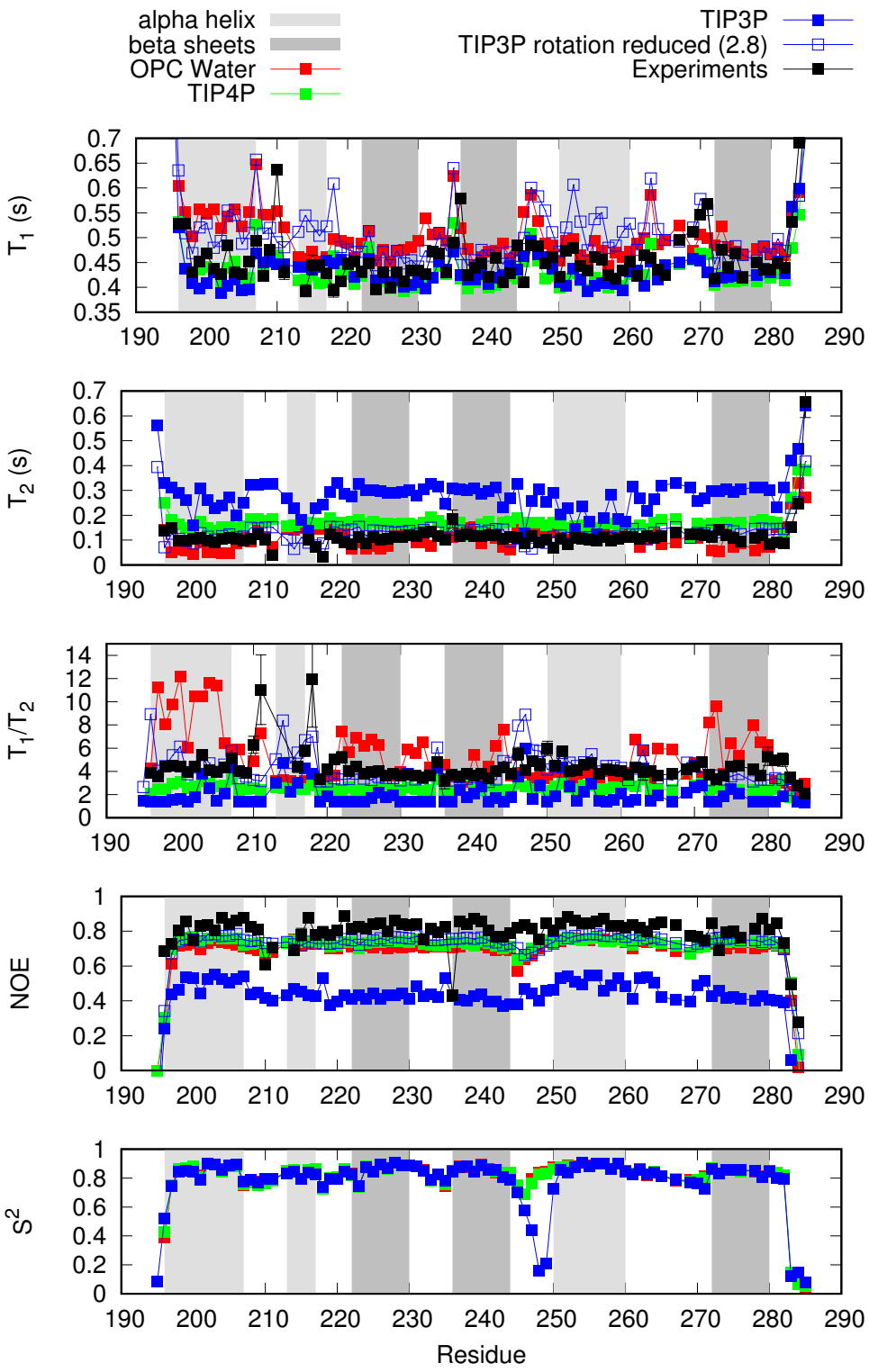

FIG. 6. Relaxation parameters for HpTonB short construct from experiments and simulations with Amber-ildn and different water models

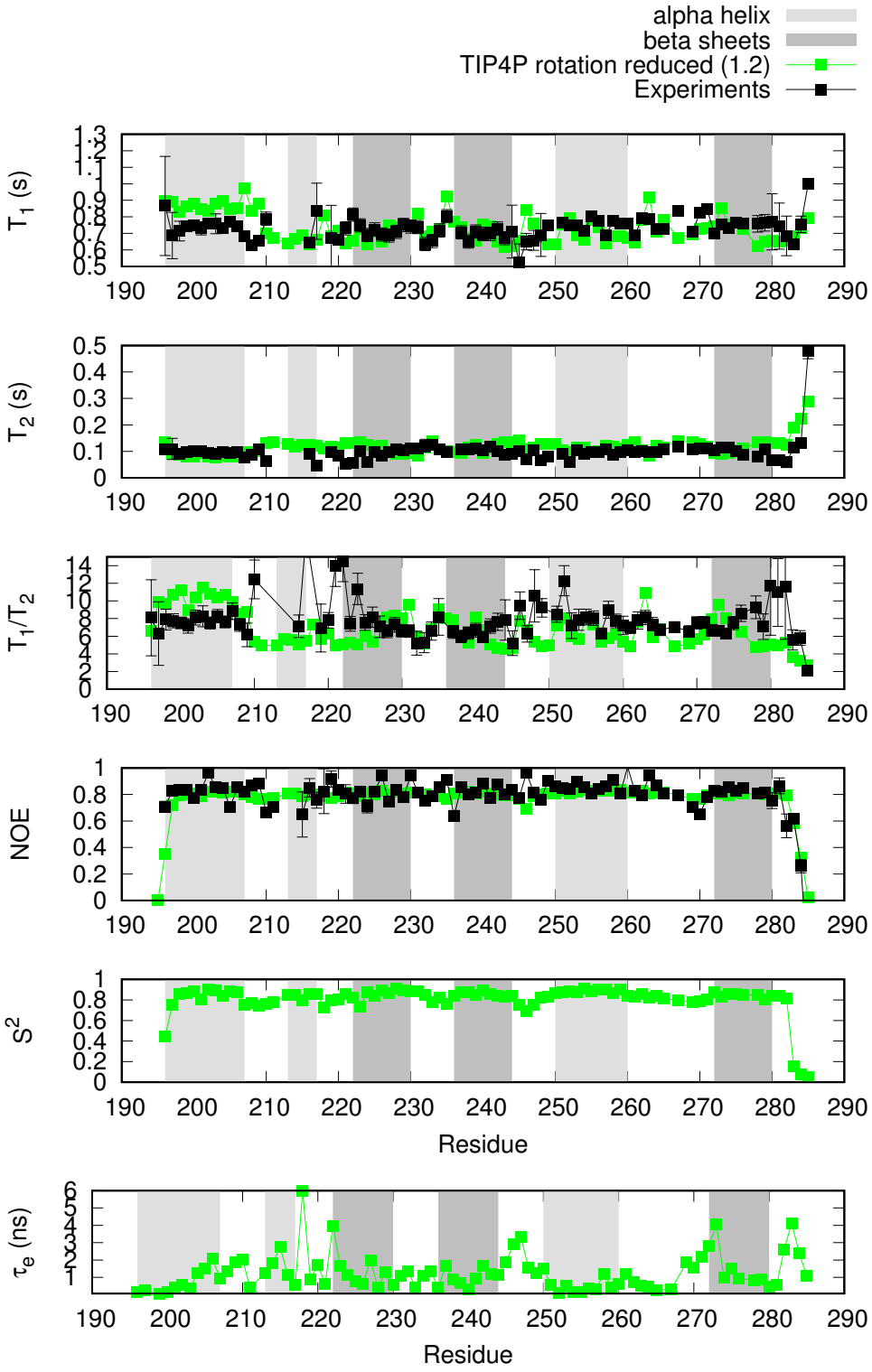

FIG. 7. Relaxation parameters for HpTonB short construct from experiments and simulations with Amber-ildn and different water models. The rotational diffusion coefficients are divided by 3.0 for tip3p simulation and by 1.3 for tip4p simulation. Experiments are done in 303K and simulations in 310K, simulations in 303K are running.

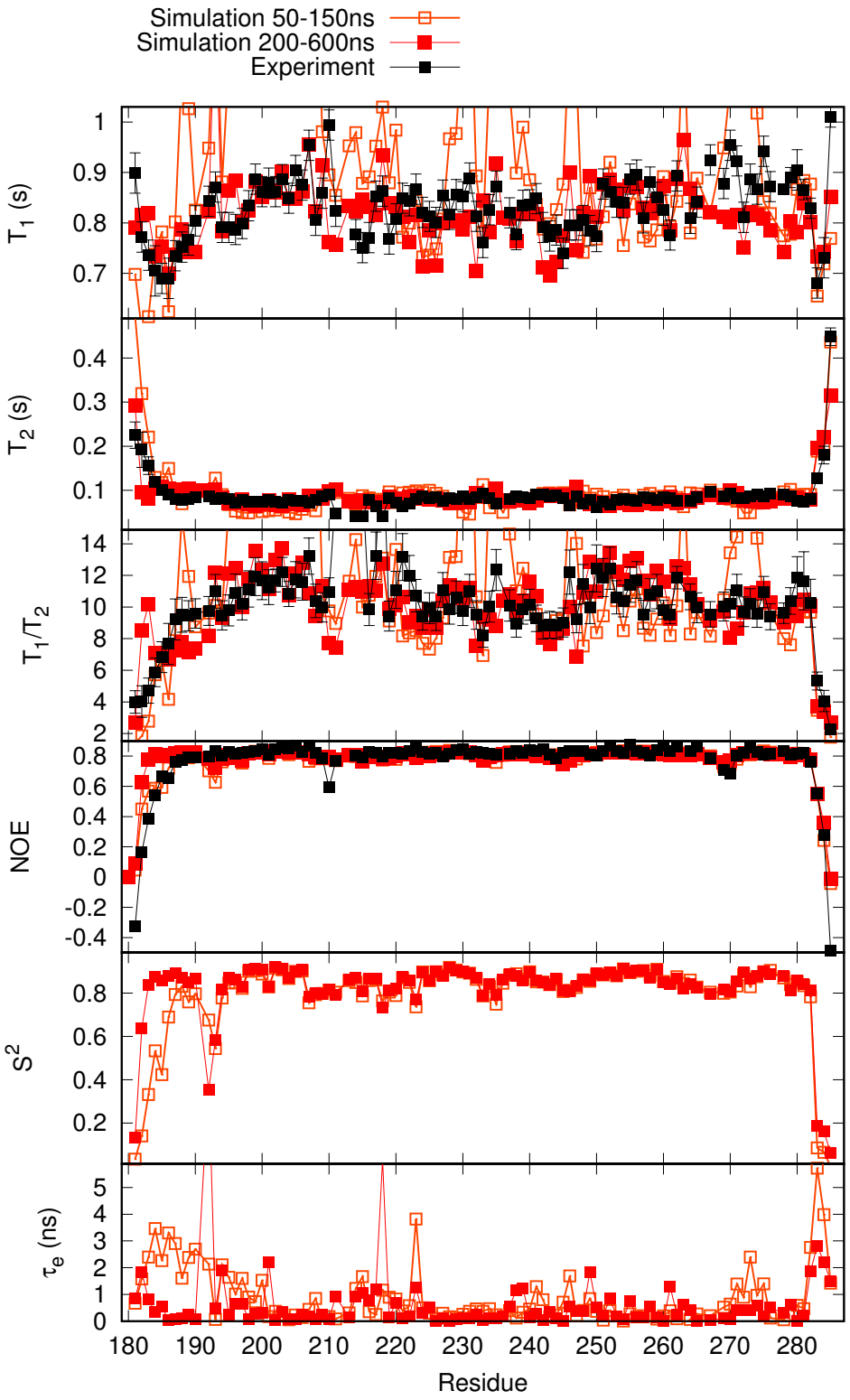

FIG. 8. PRELIMINARY RESULTS for relaxation parameters for HpTonB longer construct (107) from experiments and simulations with Amber-ildn and tip4p water models. The rotational diffusion coefficients are divided by 1.3. Experiments and simulations are done in 303K.

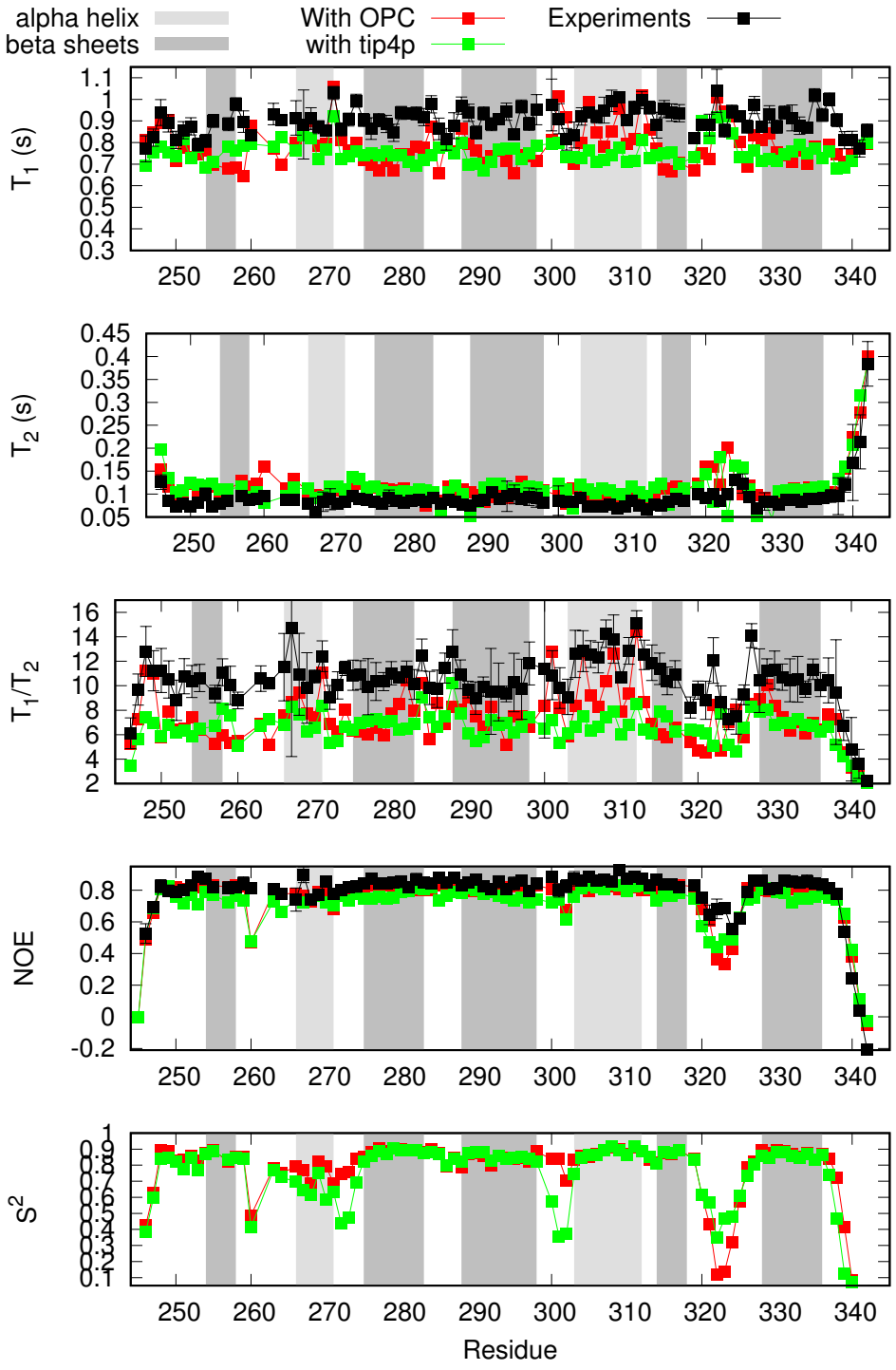

FIG. 9. Relaxation parameters for PsTonB short construct from experiments and simulations with Amber-ildn and different water models